

Double charge exchange scattering of pions by ^{18}O

L. C. Liu and Victor Franco*

Physics Department, Brooklyn College of the City University of New York, Brooklyn, New York 11210

(Received 24 September 1974)

We calculate the cross section for the double charge exchange (DCE) reaction (π^+, π^-) . The multiple-scattering series for DCE scattering of pions by nuclei is found to converge slowly. To take into account the higher order contributions, we use an eikonalized distorted wave formulation, which is obtained from the usual Glauber series by retaining those terms corresponding to coherent scattering processes. We include s , p , d , and f partial waves in the pion-nucleon (πN) elastic scattering amplitudes used in the calculations. Our results show that for incident pion energies below ~ 200 MeV the contribution of the spin-flip part of the πN elastic scattering amplitude to the cross section interferes significantly with that due to the spin-independent part of the πN amplitude. The d wave of the πN amplitude contributes significantly to the cross section above ~ 100 MeV. Above ~ 500 MeV the contribution from the f wave becomes important. The calculated total DCE cross section for $^{18}\text{O}(\pi^+, \pi^-)^{18}\text{Ne}$ has a minimum near 130 MeV. Although a maximum occurs near the (3, 3) resonance energy in both the double scattering and the double plus triple scattering cross sections, in the full distorted wave results the maximum is located near 400 MeV and is rather broad. The forward differential cross section for DCE exhibits the same qualitative features as the integrated cross section as a function of the pion incident energy. The angular distributions are peaked in the forward direction and possess structure in the form of maxima and minima or shoulders.

$$\left[\text{NUCLEAR REACTIONS } ^{18}\text{O}(\pi^+, \pi^-)^{18}\text{Ne}, E \leq 550 \text{ MeV}; \text{ calculated } \sigma(E), \right. \\ \left. \sigma(E, \theta = 0^\circ), \sigma(\theta). \right]$$

I. INTRODUCTION

Since the pion has three charge states, it can exchange two units of charge with a nucleus and still emerge as a pion. Consequently, double charge exchange (DCE) scattering of pions by nuclei, (π^+, π^-) or (π^-, π^+) , has no equivalent counterpart in nucleon-nucleus interactions. Although no definite identification of the analog state in (π^+, π^-) reactions has been made experimentally, measurements designed to do so will be performed very shortly with a π^+ beam at the Clinton P. Anderson Meson Physics Facility (LAMPF).¹

The early theoretical works in the field are double-scattering calculations.²⁻⁴ However, as we shall see, the triple and higher order multiple-scattering effects are quite significant at intermediate energies. Multiple-scattering effects have recently been studied by Kaufmann, Jackson, and Gibbs⁵ using a new formulation of the Watson theory and by Bjornenak *et al.*⁶ and by Locci and Picchi⁶ using the Glauber approximation. DCE calculations using an optical model have been done by Rost and Edwards.⁷ In the present work, we use the Glauber approximation together with a coherent scattering approximation to study the DCE scattering of positive pions by ^{18}O below

~ 550 MeV. The final nucleus ^{18}Ne is a double analog of the target nucleus ^{18}O .

The approach we take leads to a derivation of an eikonalized distorted wave approximation from the Glauber theory and represents a viable procedure for taking into account the higher order multiple-scattering effects. One of the new and useful features of the present analysis is related to our extensive use of Racah algebra which allows the antisymmetrization aspect of the scattering of pions by nucleons to be handled in a rather economical manner. We avoid using the familiar but rather lengthy method, generally employed in previous Glauber-type calculations, in which one computes the entire Slater determinant composed of the matrix elements of profile functions taken between initial and final states. In our approach we use the angular momentum algebra from the outset. We are then able to express the scattering amplitudes in terms of quantities having simple symmetry properties with respect to the values of the quantum numbers. [See Eqs. (3.3) and (3.10)]. Consequently, we can see that fewer terms than the numbers implied by the summations in those equations actually have to be computed. We can also determine which terms cancel each other. When double spin flips are involved, as in the present case, the

more conventional techniques do not provide a direct exhibition of this cancellation. Our method can be used to treat heavier nuclei for which our eikonalized distorted wave formulation may be even more appropriate.

In our calculations, we have included the effect of the spin-flip part of the elementary πN scattering amplitude. Our results show that the contribution from this part of the πN amplitude interferes significantly with that due to the spin-independent part. We have also used a more accurate parametrization of the elementary πN scattering amplitude, taking into account s , p , d , and f partial waves. In previous Glauber-type calculations, the momentum-transfer dependence of the spin-independent part of the πN amplitude was either neglected or parametrized simply by a Gaussian, and the spin-flip part of the πN amplitude was not considered. Furthermore, we have included all (A) orders of multiple scattering in our calculation since we have found some higher order terms to be significant.

In order to fully exhibit the effects of spin and of

mation by⁹ ($\hbar = 1$)

$$F_{fi}(\vec{q}) = \frac{ik'}{2\pi} \int d^2b d^3x_1 d^3x_2 \cdots d^3x_A e^{i\vec{q} \cdot \vec{b}} \delta^{(3)}\left(\frac{1}{A} \sum_{l=1}^A \vec{x}_l\right) \times \langle \pi^- | \Psi_{j'M'; T'T'_3}^*(\vec{x}_1, \dots, \vec{x}_A) \left\{ 1 - \prod_{j=1}^A [1 - \Gamma_j(\vec{b} - \vec{s}_j)] \right\} \Psi_{jM; TT_3}(\vec{x}_1, \dots, \vec{x}_A) | \pi^+ \rangle, \quad (2.1)$$

where we have used the notation $\langle \pi^- |$ and $| \pi^+ \rangle$ to denote the final and initial isospin states of the pion. The vector $\vec{q} = \vec{k} - \vec{k}'$ is the momentum transfer in the pion-nucleus center-of-mass frame. In Eq. (2.1) the profile function of the j th nucleon is defined by⁹

$$\Gamma_j(\vec{b} - \vec{s}_j) = (2\pi i k_j^*)^{-1} \int e^{-i\vec{q}' \cdot (\vec{b} - \vec{s}_j)} f(w_j, \vec{q}') d^2q', \quad (2.2)$$

where $f(w_j, \vec{q}')$ represents the on-shell πN scattering amplitude calculated at total energy w_j and at momentum transfer \vec{q}' in the pion- j th nucleon center-of-mass frame. This fundamental πN scattering amplitude has the general form^{10,11}

$$f(w_j, \vec{q}') = f^{(0)}(w_j, q') + i f^{(1)}(w_j, q') \vec{\sigma}(j) \cdot \vec{n}(j) + \vec{\Gamma} \cdot \vec{\tau}(j) [f^{(2)}(w_j, q') + i f^{(3)}(w_j, q') \vec{\sigma}(j) \cdot \vec{n}(j)]. \quad (2.3)$$

Here $\vec{\sigma}(j)$ and $\vec{\tau}(j)$ are, respectively, the spin and isospin operators which act on the spin and isospin variables of the j th nucleon. $\vec{\Gamma}$ is the pion

the higher order partial waves of the πN amplitude, we do not include in this calculation any model for nucleon-nucleon correlations or for Fermi motion. Such studies would be meaningful if the dynamical aspects of the πN off-shell amplitude were considered.

We derive the basic equations in Sec. II and calculate the double scattering contribution in Sec. III. In Sec. IV we formulate the coherent scattering approximation with the aid of a diagrammatic approach which makes the physical idea more transparent and apply it to triple scattering. By applying this approximation to triple and higher order multiple scatterings, we obtain in Sec. V an eikonalized distorted wave formula for the scattering amplitude. The results are discussed in the last section. All calculations are done in the pion-nucleus center-of-mass frame.

II. BASIC EQUATIONS

The amplitude for the double charge exchange scattering (π^+ , π^-) is given in the Glauber approxi-

isospin operator, and $\vec{n}(j)$ is defined by

$$\vec{n}(j) = (\vec{k}_j^* \times \vec{k}_j^{*'}) / k_j^* k_j^{*'}, \quad (2.4)$$

where \vec{k}_j^* and $\vec{k}_j^{*'}$ are, respectively, the initial and final pion momenta in the πN c.m. frame. The various components of the πN scattering amplitude $f^{(i)}(w_j, \vec{q}')$ ($i=0, 1, 2, 3$) are functions of the πN partial-wave phase shifts. Since the energy domain of this work corresponds to pion kinetic energies up through ~ 550 MeV, s , p , d and f waves are taken into account.

For the double charge exchange reaction



we shall be interested in calculating the transition to the ground state of ${}^{18}\text{Ne}$. This channel is of great theoretical interest since the final nucleus ${}^{18}\text{Ne}$ ($T'=1$, $T'_3=1$) is an analog state of the ${}^{18}\text{O}$ ground state. With an energy resolution of approximately 0.5 MeV this state can be well separated from the excited states of ${}^{18}\text{Ne}$.

By assuming that both the initial and the final nuclear wave functions can be described by an antisymmetrized product of single-particle harmonic oscillator wave functions, we can eliminate the

center-of-mass correlation δ function in Eq. (2.1) and write¹²

$$F_{fi}(\vec{q}) = -\frac{ik'}{2\pi} e^{q^2/4A\alpha^2} \int d^2b e^{i\vec{q}\cdot\vec{b}} \langle \pi^-; \Psi(^{18}\text{Ne}) | \prod_{j=1}^A [1 - \Gamma_j(\vec{b} - \vec{s}_j)] | \Psi(^{18}\text{O}); \pi^+ \rangle, \quad (2.6)$$

where α is the usual harmonic oscillator parameter.

In our calculations we shall use the technique of coupling and recoupling of angular momenta, adopting the convention of Fano and Racah for irreducible tensors.¹³ Accordingly, for the partial-wave decomposition of a plane wave, we write

$$e^{i\vec{q}\cdot\vec{x}} = 4\pi \sum_{l,m} Y_{lm}^*(\hat{q}) Y_m^{[l]}(\hat{x}) j_l(qx), \quad (2.7)$$

where $Y_m^{[l]}(\hat{x}) = i^l Y_{lm}(\hat{x})$. We also write

$$\begin{aligned} \vec{\sigma}(j) \cdot \vec{n}(j) &= \sum_{\lambda} (-1)^{1-\lambda} \sigma_{\lambda}^{[1]}(j) n_{-\lambda}^{[1]}(j) \\ &= \sigma_{+1}^{[1]}(j) n_{-1}^{[1]}(j) + \sigma_{-1}^{[1]}(j) n_{+1}^{[1]}(j). \end{aligned} \quad (2.8)$$

The term $n_0^{[1]}$ vanishes in the sum (2.8) since the direction of the initial momentum \vec{k}_j^* is taken along the z axis.

III. DOUBLE SCATTERING

The single scattering term in Eq. (2.1) or Eq. (2.6) gives no contribution to the DCE process.

Consequently, we may rewrite this amplitude as

$$\begin{aligned} F_{fi}^{(2)}(\vec{q}) &= F_{22}(\vec{q}) + 2F_{23}(\vec{q}) + F_{33}(\vec{q}) \\ &= K(q)(2\pi i k_1^*)^{-1} (2\pi i k_2^*)^{-1} \int d^2b d^2q_1 d^2q_2 e^{i(\vec{q} - \vec{q}_1 - \vec{q}_2) \cdot \vec{b}} \\ &\quad \times \langle (\frac{5}{2}, \frac{5}{2}) 00 | e^{i(\vec{q}_1 \cdot \vec{s}_1 + \vec{q}_2 \cdot \vec{s}_2)} [f^{(2)}(w_1, q_1) f^{(2)}(w_2, q_2) + 2i f^{(2)}(w_1, q_1) f^{(3)}(w_2, q_2) \vec{\sigma}(2) \cdot \vec{n}(2) \\ &\quad - f^{(3)}(w_1, q_1) f^{(3)}(w_2, q_2) \vec{\sigma}(1) \cdot \vec{n}(1) \vec{\sigma}(2) \cdot \vec{n}(2)] | (\frac{5}{2}, \frac{5}{2}) 00 \rangle, \end{aligned} \quad (3.2)$$

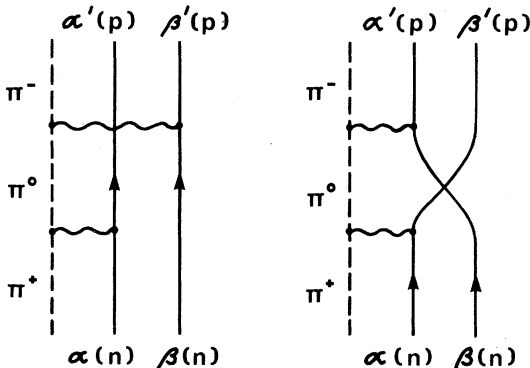


FIG. 1. Graphic representation of double scattering. The dashed line represents the pion and the solid lines represent the valence nucleons. These nucleons are regarded as "particles" with respect to the core nucleus. Their quantum numbers are denoted by Greek letters. The charge states are given by p (for proton) or n (for neutron). The wavy lines represent the $\pi N t$ matrix. The sequence of events proceeds upward.

Consequently, the leading contribution comes from double scattering. Since we are using totally antisymmetrized initial and final nuclear wave functions, we may write the double-scattering term as

$$\begin{aligned} F_{fi}^{(2)}(\vec{q}) &= -\frac{ik'}{2\pi} e^{q^2/4A\alpha^2} \sum_{\alpha, \beta, \alpha', \beta'} \int d^2b e^{i\vec{q}\cdot\vec{b}} \\ &\quad \times \langle \pi^-; \alpha' \beta' | \Gamma_1(\vec{b} - \vec{s}_1) \Gamma_2(\vec{b} - \vec{s}_2) | \alpha \beta; \pi^+ \rangle. \end{aligned} \quad (3.1)$$

Here, the quantum numbers α , β , α' , and β' run over all the permitted single-particle orbits. The states $\langle \alpha' \beta' |$ and $| \alpha \beta \rangle$ are normalized antisymmetric two-particle states.

For the specific channel (2.5) we are considering, the quantum numbers α and β can only be associated with the two $1d_{5/2}$ neutrons of ^{18}O . Similarly, the range of α' and β' is restricted to the orbits of the two $1d_{5/2}$ protons of ^{18}Ne . The situation is represented by the diagrams in Fig. 1.

where $K(q) = -ik\pi^{-1} \exp(q^2/4A\alpha^2)$. In obtaining Eq. (3.2), we have used the fact that only that part of the product $\Gamma_1 \Gamma_2$ in Eq. (3.1) which contains the factor $\vec{I} \cdot \vec{\tau}(1) \vec{I} \cdot \vec{\tau}(2)$ contributes.

The three terms defined in Eq. (3.2) represent, in successive order, the spin-independent, single spin-flip, and double spin-flip contributions. Since a spin zero final nucleus cannot be obtained from a spin zero initial nucleus by a single spin flip, the single spin-flip contribution $F_{23}(\vec{q})$ to the double scattering is zero. (This result holds for all DCE scatterings in which the final nucleus is a double analog state of the initial nucleus and both have zero spin.) We now apply the Racah algebra analysis to the remaining two terms of the amplitude $F_{fi}^{(2)}(\vec{q})$.

By using the relation (2.7) for $e^{i\vec{q}_1 \cdot \vec{s}_1}$ and for $e^{i\vec{q}_2 \cdot \vec{s}_2}$ in Eq. (3.2) we may write the spin-indepen-

dent term as

$$F_{22}(\vec{q}) = K(q) \int (-4/k_1^* k_2^*) d^2 b d^2 q_1 d^2 q_2 e^{i(\vec{q} - \vec{q}_1 - \vec{q}_2) \cdot \vec{b}} f^{(2)}(w_1, q_1) f^{(2)}(w_2, q_2) \times \sum_{l, m} C_{m-m_0}^{l l} Y_{l, m}^*(\hat{q}_1) Y_{l-m}^*(\hat{q}_2) M(l, l; q_1, q_2) \quad (3.3)$$

with

$$M(l, l; q_1, q_2) = \langle (\frac{5}{2}, \frac{5}{2}) 00 | [Y^{[l]} \otimes Y^{[l]}]_0^{[0]} j_l(q_1 x_1) j_l(q_2 x_2) | (\frac{5}{2}, \frac{5}{2}) 00 \rangle = \begin{pmatrix} \frac{5}{2} & \frac{5}{2} & 0 \\ \frac{5}{2} & \frac{5}{2} & 0 \\ l & l & 0 \end{pmatrix} \left[\langle (\frac{1}{2}, 2) \frac{5}{2} \| Y^{[l]} \| (\frac{1}{2}, 2) \frac{5}{2} \rangle \right]^2 \langle R | j_l(q_1 x_1) j_l(q_2 x_2) | R \rangle, \quad (3.4)$$

where the radial matrix elements are defined by

$$\langle R | j_l(q_1 x_1) j_l(q_2 x_2) | R \rangle \equiv \prod_{j=1}^2 \int dx x^2 j_l(q_j x) R_{n=1, l_j=2}(x) R_{n=1, l_j=2}(x). \quad (3.5)$$

Since both initial and final nuclear states have zero spin, the $(l, l)0$ angular momentum coupling scheme indicated in $M(l, l; q_1, q_2)$ is the only possible one. The harmonic oscillator radial wave function $R_{n, \lambda}(x)$ is given by

$$R_{n=1, \lambda}(x) = \frac{\alpha^{3/2}}{\pi^{1/4}} \left(\frac{2^{\lambda+2}}{(2\lambda+1)!} \right)^{1/2} (\alpha x)^\lambda e^{-\alpha^2 x^2/2}. \quad (3.6)$$

We should point out that the form (3.4) is quite general in the sense that the radial wave functions R needed in the evaluation of Eq. (3.5) is not restricted to harmonic oscillator functions. Any single-particle shell model wave function can be used, provided that an appropriate c.m. correlation correction is made. By using

$$Y_{l, m}^*(\hat{q}) = \left(\frac{2l+1}{4\pi} \frac{(l-m)!}{(l+m)!} \right)^{1/2} P_l^m(0) e^{-im\phi_q}, \quad (3.7)$$

we obtain

$$F_{22}(\vec{q}) = 12\pi K(q) \int db b J_0(qb) \sum_{l=0,2,4} \sum_{-l \leq m \leq l} (-1)^m \begin{pmatrix} \frac{5}{2} & l & \frac{5}{2} \\ -\frac{1}{2} & 0 & \frac{1}{2} \end{pmatrix}^2 (2l+1) I^{(22)}(l, m; l, -m; b), \quad (3.8)$$

where we have defined

$$I^{(22)}(l, m; l, -m; b) = -(k_1^* k_2^*)^{-1} \int dq_1 dq_2 q_1 q_2 f^{(2)}(w_1, q_1) f^{(2)}(w_2, q_2) \times J_m(q_1 b) J_{-m}(q_2 b) P_l^m(0) P_l^{-m}(0) \langle R | j_l(q_1 x_1) j_l(q_2 x_2) | R \rangle. \quad (3.9)$$

Similarly, after some algebra the double spin-flip part can be reduced to

$$F_{33}(\vec{q}) = K(q) \int d^2 b e^{i\vec{q} \cdot \vec{b}} 16\pi^2 \sum_{l=0,2,4} \sum_{L=l \pm 1} \sum_{l'=l, l \pm 2} \sum_{m, m'} (-1)^{L+m} (2L+1)^{-1} \times \{ C_{l m m+1}^{1 l l} [C_{l m' l-m-1}^{1 l' l} I_{--}^{(33)}(l, m; l', m'; L; b) + C_{-l m' l-m-1}^{1 l' l} I_{-+}^{(33)}(l, m; l', m'; L; b)] + C_{-l m m-1}^{1 l l} [C_{l m' l-m+1}^{1 l' l} I_{+-}^{(33)}(l, m; l', m'; L; b) + C_{-l m' l-m+1}^{1 l' l} I_{++}^{(33)}(l, m; l', m'; L; b)] \}, \quad (3.10)$$

where the function $I_{\pm}^{(33)}$ is defined by

$$\begin{aligned}
 I_{\pm}^{(33)}(l, m; l' m'; b) = & - (k_1^* k_2^*)^{-1} \left[i^{-l-(m+1)} 30 \left(\frac{2l+1}{4\pi} \right)^{3/2} \left(\frac{(l-m)!}{(l+m)!} \right)^{1/2} \right] \left[i^{-l'-(m'-1)} 30 \left(\frac{2l'+1}{4\pi} \right)^{3/2} \left(\frac{(l'-m')!}{(l'+m')!} \right)^{1/2} \right] \\
 & \times \int d q_1 d q_2 q_1 q_2 f^{(3)}(w_1, q_1) J_{m+1}(q_1 b) P_l^m(0) \begin{pmatrix} 2 & l & 2 \\ 0 & 0 & 0 \end{pmatrix} \begin{pmatrix} \frac{1}{2} & 2 & \frac{5}{2} \\ \frac{1}{2} & 2 & \frac{5}{2} \\ 1 & l & L \end{pmatrix} f^{(3)}(w_2, q_2) J_{m'-1}(q_2 b) P_{l'}^{m'}(0) \\
 & \times \begin{pmatrix} 2 & l' & 2 \\ 0 & 0 & 0 \end{pmatrix} \begin{pmatrix} \frac{1}{2} & 2 & \frac{5}{2} \\ \frac{1}{2} & 2 & \frac{5}{2} \\ 1 & l' & L \end{pmatrix} \langle R | j_i(q_1 x_1) j_{i'}(q_2 x_2) | R \rangle. \quad (3.11)
 \end{aligned}$$

The subscript + in $I_{\pm}^{(33)}$ corresponds to the subscript $m+1$ of the first Bessel function in this equation and to the exponent $m+1$; the subscript - corresponds to the subscript $m'-1$ of the second Bessel function and to the exponent $m'-1$. There are similar expressions for $I_{\pm}^{(33)}$, $I_{\pm}^{(33)}$, and $I_{\pm}^{(33)}$. These are obtained by making the corresponding changes of the + and - signs in the subscripts and exponents $m+1$ and $m'-1$ in $I_{\pm}^{(33)}$.

IV. TRIPLE SCATTERING

The triple-scattering contribution in the Glauber approximation is given by

$$F_{fi}^{(3)}(\vec{q}) = \frac{i k'}{2\pi} e^{a^2/4A\alpha^2} \sum_{\alpha\beta\gamma\alpha'\beta'\gamma'} \int d^2\vec{b} e^{i\vec{q}\cdot\vec{b}} \langle \pi^- | \langle \alpha' \beta' \gamma' | \Gamma_3(\vec{b} - \vec{s}_3) \Gamma_2(\vec{b} - \vec{s}_2) \Gamma_1(\vec{b} - \vec{s}_1) | \alpha \beta \gamma \rangle | \pi^+ \rangle, \quad (4.1)$$

where $\langle \alpha' \beta' \gamma' |$ and $| \alpha \beta \gamma \rangle$ stand, respectively, for antisymmetrized final and initial three-nucleon states. In Glauber theory, the pion can scatter off any nucleon only once. It follows that for the specific channel (2.5) being studied, after assigning the quantum numbers α' , β' , α , and β to the valence nucleons, we must have the restriction $\gamma' = \gamma$, with γ spanning all orbits occupied by the core nucleons. In order to exhibit all possible different intermediate charge exchange sequences, we express the matrix element in Eq. (4.1) as

$$\begin{aligned}
 \frac{1}{3} \langle \pi^- | [& \langle \alpha' \beta' | \Gamma_3 \Gamma_2 | \alpha \beta \rangle \langle \gamma | \Gamma_1 | \gamma \rangle + \langle \alpha' \beta' | \Gamma_3 \Gamma_1 | \alpha \beta \rangle \langle \gamma | \Gamma_2 | \gamma \rangle + \langle \gamma | \Gamma_3 | \gamma \rangle \langle \alpha' \beta' | \Gamma_2 \Gamma_1 | \alpha \beta \rangle \\
 & + \langle \alpha' | \Gamma_3 | \gamma \rangle \langle \beta' \gamma | \Gamma_2 \Gamma_1 | \alpha \beta \rangle + \langle \beta' | \Gamma_3 | \gamma \rangle \langle \gamma \alpha' | \Gamma_2 \Gamma_1 | \alpha \beta \rangle + \langle \beta' \gamma | \Gamma_3 \Gamma_1 | \alpha \beta \rangle \langle \alpha' | \Gamma_2 | \gamma \rangle \\
 & + \langle \gamma \alpha' | \Gamma_3 \Gamma_1 | \alpha \beta \rangle \langle \beta | \Gamma_2 | \gamma \rangle + \langle \gamma \alpha' | \Gamma_3 \Gamma_2 | \alpha \beta \rangle \langle \beta' | \Gamma_1 | \gamma \rangle + \langle \beta' \gamma | \Gamma_3 \Gamma_2 | \alpha \beta \rangle \langle \alpha' | \Gamma_1 | \gamma \rangle] | \pi^+ \rangle, \quad (4.2)
 \end{aligned}$$

where the argument $\vec{b} - \vec{s}_j$ of the profile function Γ_j is understood. The symbols $| \alpha \beta \rangle$ etc. denote normalized antisymmetrized two-nucleon states and $| \gamma \rangle$ etc. the normalized single-nucleon states. The sequence is ordered according to the indices of the Γ 's.

The first three terms in (4.2) correspond to three different sequences all having the pion scattered elastically by a core nucleon. Those processes represent the coherent scattering of the pion from the core nucleus, and are shown graphically in Figs. 2(a)–2(c). The fourth and fifth terms are forbidden by the Pauli principle, as are two of the four contributions arising from the sixth and seventh terms. The remaining matrix elements all involve exchanges between valence and core nucleons. A core nucleon is first excited into the $d_{5/2}$ proton orbit and the hole left in the core nucleus is then removed by the deexcitation of a $d_{5/2}$ neutron. These processes are shown in

Figs. 2(d)–2(f). We see that different sequences of creating and annihilating the hole state give different charge exchange sequences and hence different transition strengths. These third-order diagrams can be obtained from the second-order diagrams (Fig. 1) by inserting into the latter the diagram elements shown in Fig. 3. We insert the points indicated by the \times 's at all possible sequences, and annihilate the hole states in all possible ways such that the pion interacts once with each nucleon (Glauber approximation), charge is conserved at each interaction vertex, and no two nucleons occupy the same orbit (Pauli principle).

Terms involving exchange between valence and core nucleons are, in general, expected to be much less important than the coherent terms, since two intermediate orbit changes (inelastic scattering) for nucleons are involved. We therefore define a "coherent scattering approximation" by neglecting the terms involving exchange be-

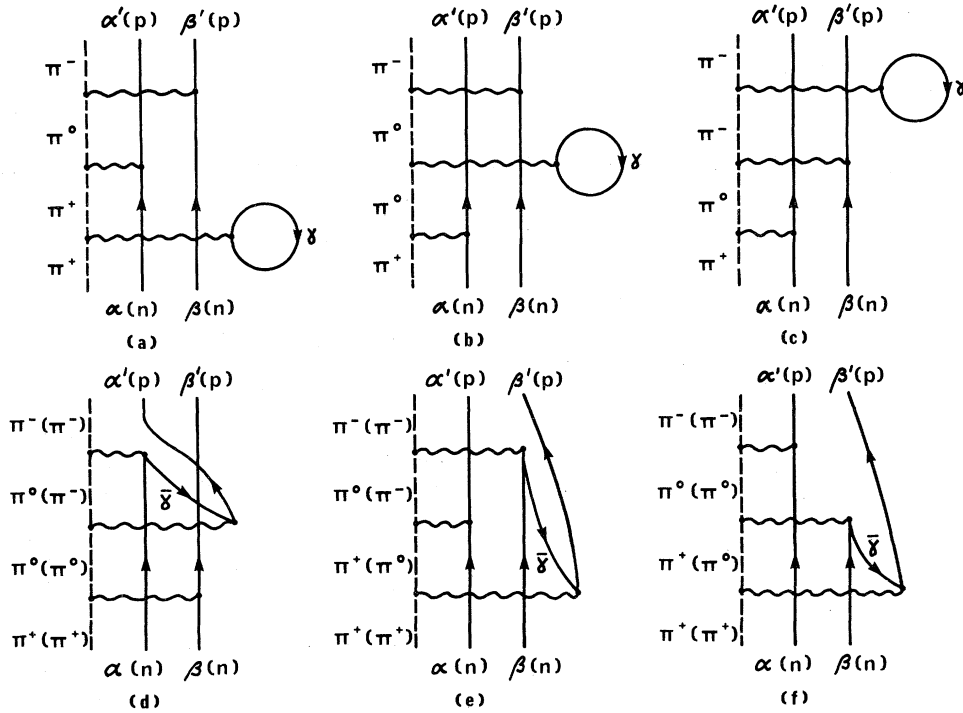


FIG. 2. Diagrams representing possible triple scatterings. The notation is the same as for Fig. 1. A line with an arrow pointing downward denotes the hole state $\bar{\gamma}$ (conjugate to the particle state of quantum number γ). The charge state of the pion corresponding to intermediate processes involving a neutron hole are indicated in the parentheses to the right of those corresponding to intermediate processes involving a proton hole. All diagrams should be supplemented by diagrams with α and β interchanged or with α' and β' interchanged.

tween the valence and core nucleons. We obtain in this approximation

$$F_{fi}^{(3)}(\vec{q}) \approx -K(q) \int d^2b e^{i\vec{q}\cdot\vec{b}} [\bar{F}_{22}(b) + \bar{F}_{33}(b)] (2\pi i k_3^*)^{-1} \times \int d^2q_3 e^{-i\vec{q}_3\cdot\vec{b}} \sum_{\gamma} \langle \gamma | f(w_3, \vec{q}_3) e^{i\vec{q}_3\cdot\vec{s}_3} | \gamma \rangle, \tag{4.3}$$

where

$$\sum_{\gamma} \langle \gamma | f(w_3, q_3) e^{i\vec{q}_3\cdot\vec{s}_3} | \gamma \rangle = f^{(0)}(w_3, q_3) \rho_c(\vec{q}_3).$$

For the ¹⁶O core, we use¹⁴

$$\rho_c(\vec{q}) = \sum_{\gamma} \langle \gamma | e^{i\vec{q}\cdot\vec{x}} | \gamma \rangle = 16(1 - q^2/8\alpha^2) e^{-q^2/4\alpha^2}. \tag{4.4}$$

The quantities $\bar{F}_{22}(b)$ and $\bar{F}_{33}(b)$ in Eq. (4.3) are, respectively, the integrands of the d^2b integration in Eqs. (3.3) and (3.10).

V. HIGHER ORDER CONTRIBUTIONS

The fourth order diagrams can be obtained from the third order diagrams by applying our graphic

rules. As an illustration, in Fig. 4 we present all fourth order diagrams generated from the diagram in Fig. 2(a).

The higher the order of multiple scattering, the more involved are the diagrams. Clearly, some approximation is desirable to make the calculation tractable. In view of the expected smallness of the contribution involving the excitation of a core nucleon and the subsequent deexcitation of another nucleon to fill the hole in the core, we have applied the "coherent scattering approximation" to all orders. This is equivalent to ignoring diagrams containing the element shown in Fig. 3(b).

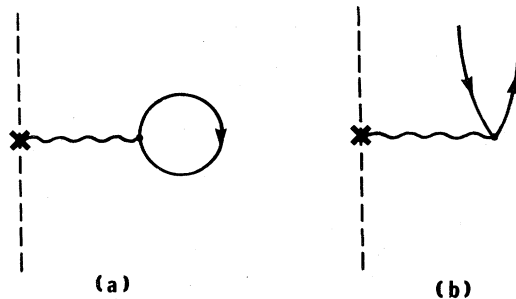


FIG. 3. Diagram elements needed for insertion into Fig. 1 to obtain Fig. 2.

The total scattering amplitude becomes

$$\begin{aligned}
 F_{fi}^{cs}(\vec{q}) = & \frac{-ik'}{2\pi} e^{\alpha^2/4A\alpha^2} \frac{1}{3} \sum_{\alpha\beta\alpha'\beta'} \int d^2b e^{i\vec{q}\cdot\vec{b}} \\
 & \times \langle \pi^- | \left\{ \langle \alpha' \beta' | \Gamma_1(\vec{b} - \vec{s}_1) \Gamma_2(\vec{b} - \vec{s}_2) | \alpha \beta \rangle \langle \psi(^{16}\text{O}) | \exp \left[i \sum_{j=3}^A \chi_j(\vec{b} - \vec{s}_j) \right] | \psi(^{16}\text{O}) \rangle \right. \\
 & + \langle \alpha' \beta' | \Gamma_1(\vec{b} - \vec{s}_1) \langle \psi(^{16}\text{O}) | \exp \left[i \sum_{j=3}^A \chi_j(\vec{b} - \vec{s}_j) \right] | \psi(^{16}\text{O}) \rangle \Gamma_2(\vec{b} - \vec{s}_2) | \alpha \beta \rangle \\
 & \left. + \langle \psi(^{16}\text{O}) | \exp \left[i \sum_{j=3}^A \chi_j(\vec{b} - \vec{s}_j) \right] | \psi(^{16}\text{O}) \rangle \langle \alpha' \beta' | \Gamma_1(\vec{b} - \vec{s}_1) \Gamma_2(\vec{b} - \vec{s}_2) | \alpha \beta \rangle \right\} | \pi^+ \rangle . \quad (5.1)
 \end{aligned}$$

For a core nucleus as heavy as ^{16}O , we take the optical limit to describe the scattering of pions by the core nucleus and write

$$\langle \psi(^{16}\text{O}) | \exp \left[\sum_{j=3}^A i \chi_j(\vec{b} - \vec{s}_j) \right] | \psi(^{16}\text{O}) \rangle \approx e^{i \chi_c(\vec{k}, \vec{b})} , \quad (5.2)$$

where

$$\chi_c(\vec{k}; \vec{b}) = \frac{-i}{2k} \int_{-\infty}^{+\infty} \bar{U}_{\text{opt}, \vec{k}}(\vec{b}, z) dz . \quad (5.3)$$

It is worth pointing out that the larger the number of nucleons in the core nucleus, the better the optical description represented by Eq. (5.2). The bar on the optical potential \bar{U}_{opt} in Eq. (5.3) denotes that for the general case where the spin and isospin of the core nucleus are different from zero, a mean value of the optical potential must

be taken over the three pion-charge states. In the case of a zero spin and zero isospin core nucleus, as is the case with ^{16}O , this notation is somewhat redundant. In this calculation, we use a local potential which has the following structure

$$\bar{U}_{\text{opt}}(k, \vec{r}) = -4\pi J \bar{f}_{\pi N}(k^*, -\vec{\nabla}^2) \rho_c(\vec{r}) , \quad (5.4)$$

where the Jacobian J transforms the πN scattering amplitude from the πN c.m. frame to the π -nucleus c.m. frame. In our eikonal formulation, the pion predominantly undergoes small angle scattering. Consequently, we set $J = k/k^*$, and the operator $-\vec{\nabla}^2$ in Eq. (5.4) is related to the pion momentum transfers in the π -nucleus and πN c.m. frames by $-\vec{\nabla}^2 = \vec{q}^2 \approx \vec{q}^{*2}$. Hence for a spin-zero isospin-zero core nucleus, as is the case with ^{16}O , we have the following operator form for the πN amplitude in

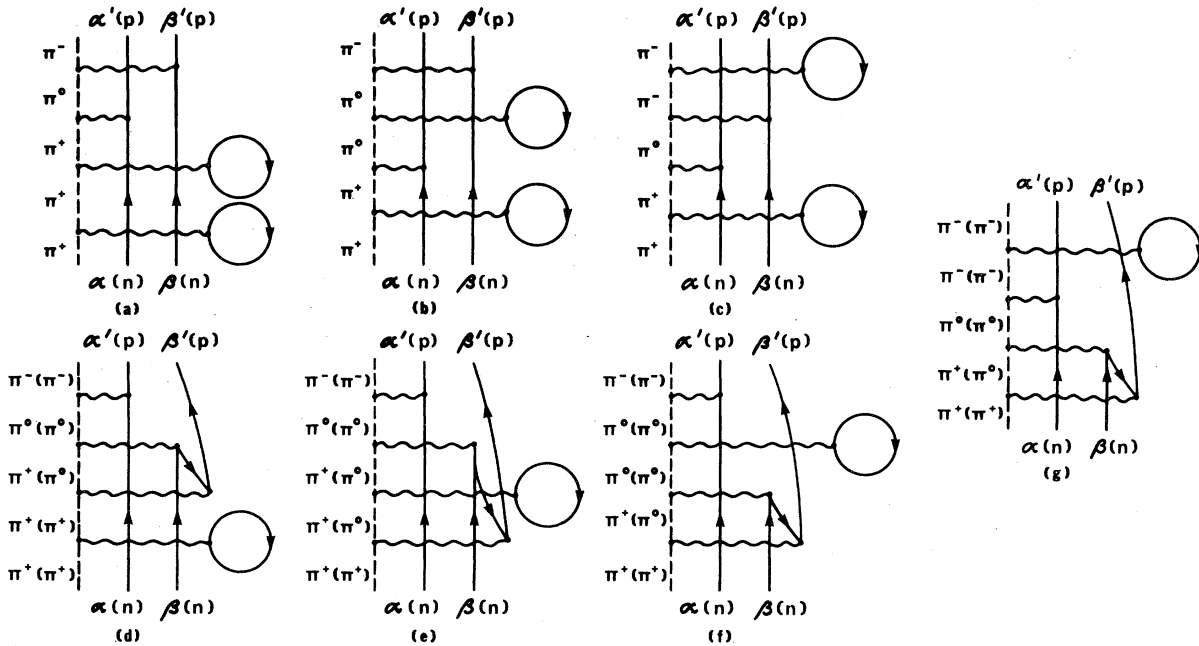


FIG. 4. Sample diagrams for quadruple scattering, generated by the diagram of Fig. 2 (a). The notation is the same as for Fig. 1.

coordinate space:

$$\begin{aligned} \bar{f}_{\pi N}(k^*, -\vec{\nabla}^2) &= f^{(0)}(k^*, -\vec{\nabla}^2) \\ &= (A_s^{(0)} + A_p^{(0)} + A_d^{(0)} + A_f^{(0)}) + (A_p^{(0)} + 3A_d^{(0)} + 6A_f^{(0)}) (\vec{\nabla}^2/2k^{*2}) \\ &\quad + (1.5A_d^{(0)} + 7.5A_f^{(0)}) (\vec{\nabla}^2/2k^{*2})^2 \\ &\quad + 2.5A_f^{(0)} (\vec{\nabla}^2/2k^{*2})^3. \end{aligned} \quad (5.5)$$

The $A^{(0)}$'s are related to the various πN partial-wave amplitudes, $a_{2T,2J}^l(k^*) = \{\eta_{2T,2J}^l(k^*) \exp[2i\delta_{2T,2J}^l(k^*)] - 1\}/2ik^*$, by the equations

$$\begin{aligned} A_s^{(0)} &= \frac{1}{3}(2a_{31}^0 + a_{11}^0), \\ A_p^{(0)} &= \frac{1}{3}(2a_{31}^1 + 4a_{33}^1 + a_{11}^1 + 2a_{13}^1), \\ A_d^{(0)} &= \frac{1}{3}(4a_{33}^2 + 6a_{35}^2 + 2a_{13}^2 + 3a_{15}^2), \\ A_f^{(0)} &= \frac{1}{3}(6a_{35}^3 + 8a_{37}^3 + 3a_{15}^3 + 4a_{17}^3). \end{aligned} \quad (5.6)$$

They represent, respectively, the s , p , d , and f wave contribution to the scalar part of πN amplitude $f^{(0)}$. Clearly, if we neglect the d and f waves, then $A_d^{(0)} = A_f^{(0)} = 0$ in Eq. (5.5), and the optical potential will reduce to the simpler but more widely employed local Laplacian form.¹⁵

The amplitude $F_{fi}^{cs}(\vec{q})$ has the familiar "distorted wave" form with the double-scattering operator $\Gamma_1\Gamma_2$ corresponding to scattering of the pion from the valence neutron pair acting as the fundamental interaction.

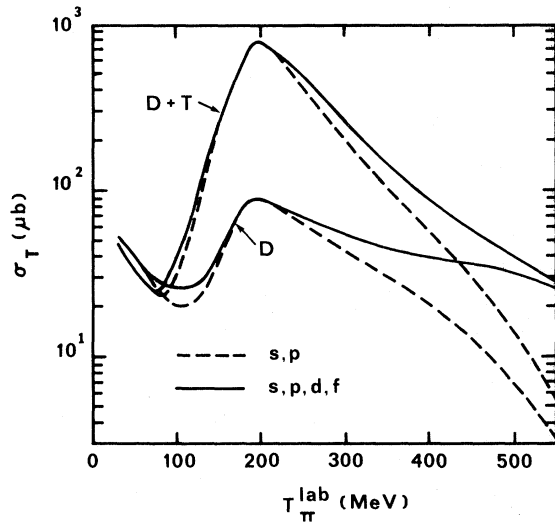


FIG. 5. The total DCE cross sections $^{18}\text{O}(\pi^+, \pi^-)^{18}\text{Ne}$ due to the double-scattering (D) and the double-plus-triple-scattering (D+T) contributions as function of incident pion kinetic energy. The dashed curves represent the results with only s and p waves of the πN amplitude taken into account. The solid curves represent the results containing s , p , d , and f waves of the πN amplitude.

VI. NUMERICAL RESULTS AND DISCUSSION

In all calculations the CERN "theoretical" fit¹⁶ was used for the πN amplitudes $f^{(i)}$. Since no data exist for the DCE reaction and since we are mainly interested in the qualitative features of the calculations, rather than the detailed numerical results, we have not investigated the effects of uncertainties of the πN phase shifts on the numerical values we obtain. The \vec{q}' dependence of the πN scattering amplitude (2.3) is essentially of two types, namely, $\cos\theta_j^* = \hat{k}_j^* \cdot \hat{k}_{j'}^*$ and $|\hat{k}_j^* \times \hat{k}_{j'}^*|$. We have used the relations $\hat{k}_j^* \cdot \hat{k}_{j'}^* = (\mathbb{K}_j^{*2} + \mathbb{K}_{j'}^{*2} - \vec{q}'^2)/2k_j^*k_{j'}^*$ and $|\hat{k}_j^* \times \hat{k}_{j'}^*| \simeq q'/k_j^*$ to extrapolate $f(\omega_j, \vec{q}')$ to the unphysical region. The first relation is exact. The second relation is an approximation which represents the quantity $|\hat{k}_j^* \times \hat{k}_{j'}^*|$ fairly well for small values of q' and allows the integration defining the nucleon profile function to be carried out in the region of unphysical q' . Using these relations with a partial wave expansion is perhaps

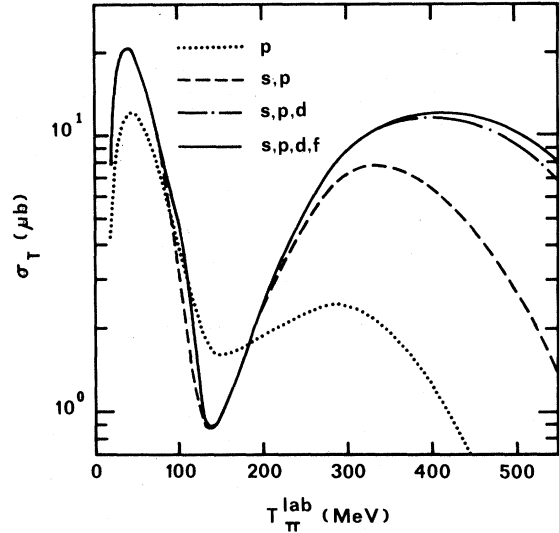


FIG. 6. The total DCE cross section $^{18}\text{O}(\pi^+, \pi^-)^{18}\text{Ne}$ given by the full calculation. The dashed and solid curves have the same description as for Fig. 5. The dash-dotted curve represents the results with the s , p , and d waves of the πN amplitude included and cannot be distinguished graphically from the solid curve for energies below 350 MeV. The dotted curve represents the results due to the p wave only.

more realistic than using a Gaussian parametrization at energies below 550 MeV and near the (3,3) resonance in particular. The harmonic oscillator parameter α was taken to be 0.5656 fm^{-1} . This value is based upon the electron scattering data,¹⁴ with the finite size of the proton being corrected for.

In Figs. 5 and 6 we present the integrated DCE cross section as a function of the pion kinetic energy. In Fig. 5 we compare the cross sections for only double scattering with those for double plus triple scattering. We also compare these cross sections when only s and p waves are considered with those when s , p , d , and f waves are considered. We see that above 100 MeV the cross section obtained from the double-plus-triple-scattering contributions is considerably greater than that obtained from only double scattering; indicating that a double-scattering approximation is not a valid one. In Fig. 6 we present the full calculation, showing the result obtained when only p wave, when only s and p waves, when only s , p , and d waves, and when s , p , d , and f waves are considered. We see that the full calculation yields a cross section that is considerably smaller than those for double or double plus triple scattering, indicating the multiple-scattering series converges rather slowly.¹⁷ Although the integrated cross sections due to the double-scattering contribution and the double-plus-triple-scattering contribution, shown in Fig. 5, exhibit a *maximum* near the (3,3) resonance energy, this characteristic peak structure disappears in the full calculation result. The distortion shifts the maximum to approximately 400 MeV and makes it rather broad. In addition, there is a deep minimum near 130 MeV. The presence of this minimum is due to the strong in-

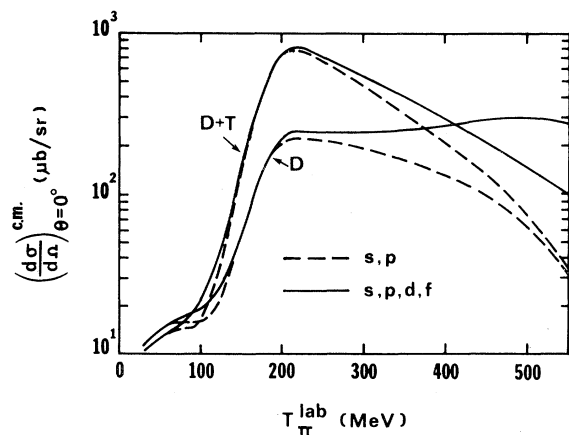


FIG. 7. The $^{18}\text{O}(\pi^+, \pi^-)^{18}\text{Ne}$ forward differential cross sections due to the double-scattering (D) and the double-plus-triple-scattering (D+T) contributions. Same description as for Fig. 5.

terference between the πN s and p waves on the one hand and the multiple-scattering effects on the other. By inspecting the dotted curves in Fig. 6 we see that when only the p wave is considered, the cross section exhibits a shallow minimum near 150 MeV and does not vary rapidly between ~ 100 to 400 MeV. On the other hand, the dashed curve that includes both the s and p waves exhibits a sharp minimum near 130 MeV. The effect of the interference between the s and p waves is to shift the minimum downward by ~ 20 MeV and to greatly increase its sharpness. The energy region of the sharp minimum corresponds to the P_{33} πN resonance energy inside a finite nucleus. At this energy, the attenuation of the pion wave by the distortion becomes very strong and helps to produce the minimum in the cross section. Between 130 and 400 MeV the cross section increases by more than a factor of 10.

It is worth pointing out that our results show clearly that for this reaction, the d wave contribution of the elementary πN amplitude is very important. Although the inclusion of the d wave hardly alters the numerical results in the energy region 150 to 250 MeV, it increases the cross sections at higher energies significantly. The cross sections in the energy region around 100 MeV are also enhanced by the d wave contribution. It has long been argued that in this region the d wave need not be considered as a result of the small-

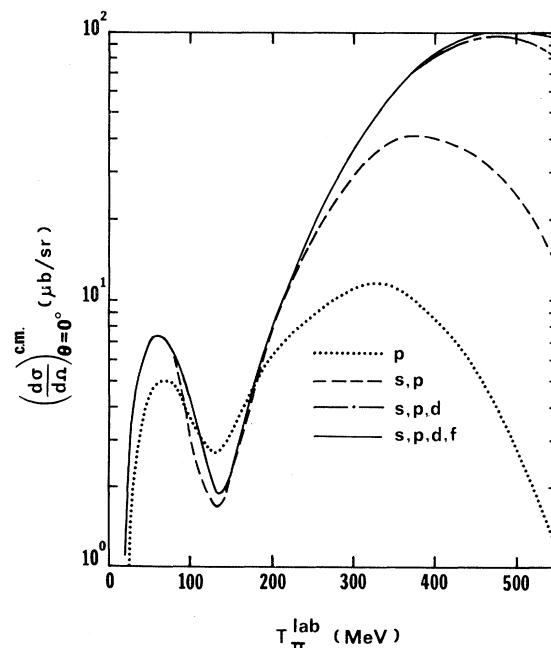


FIG. 8. The $^{18}\text{O}(\pi^+, \pi^-)^{18}\text{Ne}$ forward differential cross sections given by the full distorted wave calculation. Same description as for Fig. 6.

ness of its phase shifts. However, we find that while the phase shifts are small in this region, the d wave part brings into the πN amplitude a term proportional to $(\cos\theta^*)^2$, which, when expressed in terms of the three-momentum transfer \vec{q}' of the pion, introduces a \vec{q}'^4 component into the πN scattering amplitude in momentum space. In fact this \vec{q}'^4 term make a non-negligible contribution to the total DCE cross section via the profile function defined in Eq. (2.2). In the integration of this function, if only s and p waves were retained, the integrand $f(\omega, \vec{q}')$ would involve terms only up to \vec{q}'^2 . We have seen that the inclusion of the d wave also affects the distorting potential U_{opt} by introducing a $\vec{\nabla}^4$ term.

We have examined the effect of the core density on the cross sections. Our results show that if we increase the core radius of the nucleus, the total DCE cross sections decrease. The general trend is that the higher the pion energy, the smaller the decrease. Furthermore, the deep minimum shifts toward lower energies. For example, if we increase the radius by 11 and 25%, the position of the minimum shifts from the original value of ~ 130 MeV to ~ 120 and ~ 110 MeV, respectively.

In Fig. 7 we present the forward differential DCE cross sections due to the double-scattering contribution and the double-plus-triple-scattering contribution. The calculations were done with s and p waves and with s , p , d , and f waves. We see that above 200 MeV one must include more than just the s and p waves in the calculation. In

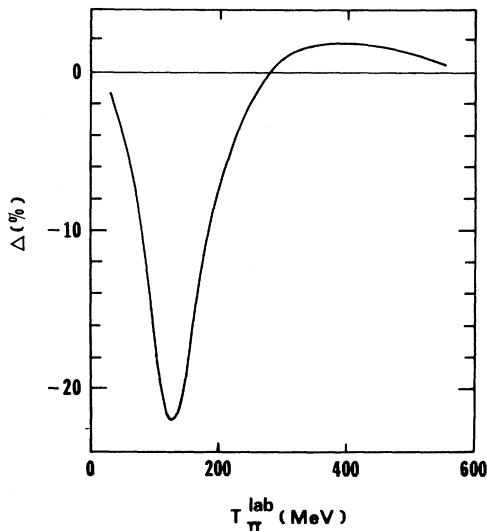


FIG. 9. The influence of the spin-flip part of the πN amplitude on the total DCE cross section as function of pion energy. The quantity Δ is defined in the text. All s , p , d , and f waves of the πN amplitude are considered.

Fig. 8 we show the complete calculation for the forward differential cross sections. As in the integrated cross section case, we see that the d wave is important near 100 MeV and above 250 MeV.

In Fig. 9 we show the interference effect between the amplitudes $F_{22}^{cs}(0)$ and $F_{33}^{cs}(0)$, which are, respectively, connected to the spin-independent and the double spin-flip parts of the elementary πN amplitude. We have introduced a quantity Δ defined by

$$\Delta = [|F_{22}^{cs}(0) + F_{33}^{cs}(0)|^2 - |F_{22}^{cs}(0)|^2] / |F_{22}^{cs}(0)|^2.$$

The positive and negative sign of this number therefore represents, respectively, the constructive and destructive interference effect of these two amplitudes. Our results show that they are destructive below ~ 300 MeV and the maximum effect occurs near 130 MeV, the energy at which the integrated cross section has its minimum. Figure 9 indicates clearly that at pion energies between 80 and 180 MeV the spin-flip part of the πN scattering amplitude should be included in calculations.

In Figs. 10 and 11, we show the differential cross sections at 130 and 450 MeV. They are both peaked forward and possess structure in the form of shoulders, or maxima and minima. The shapes are not altered significantly by the inclusion of spin flip or d and f wave scattering of the πN am-

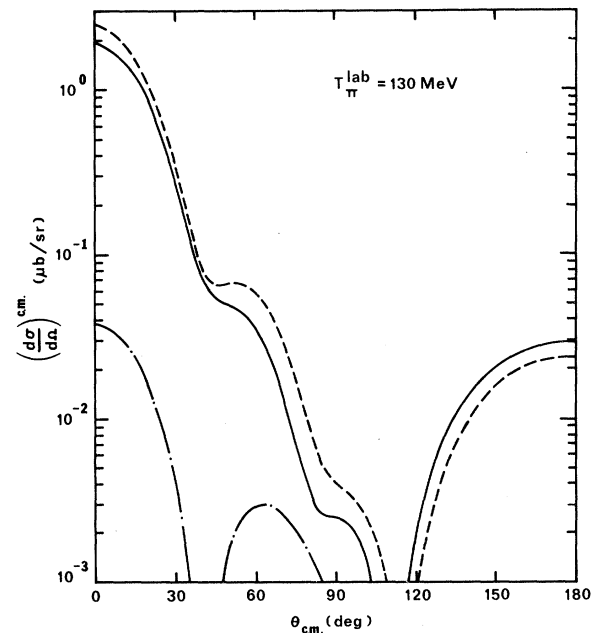


FIG. 10. The DCE differential cross section (solid curve) at 130 MeV. The dashed curve is given by $F_{22}^{cs}(\vec{q})$ alone, while the dash-dotted curve is given by $F_{33}^{cs}(\vec{q})$ alone.

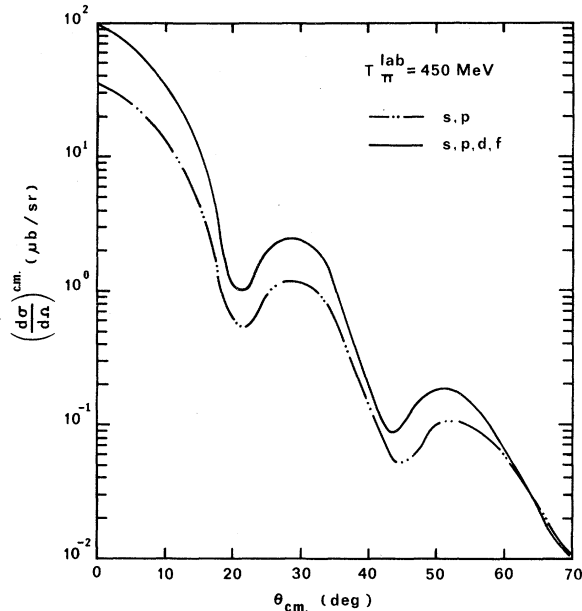


FIG. 11. The DCE differential cross section at 450 MeV. The solid curve contains s , p , d , and f waves of πN scattering. The dash-double-dotted curve contains only s and p waves of πN scattering.

plitude. However, the magnitudes are affected considerably.

The results obtained from pion-nucleus elastic scattering calculations show that the Glauber approximation is in reasonable agreement with the measurements for pion energies above 120 MeV.¹⁸ Consequently, our numerical results for energies below 120 MeV should only be regarded as qualitative. Because of the complexity of the problem different approximations have been used in the various published calculations; these models will be tested by the measurements that will soon be made. However, our conclusions on the convergence properties of the multiple-scattering series, on the influence of spin, and on the significance of the d and f waves appear to be quite general and should not be altered by more detailed calculations.

ACKNOWLEDGMENTS

We thank Mr. Girish K. Varma for useful information. One of us (V.F.) thanks Dr. William R. Gibbs and group T-5 for their hospitality at Los Alamos Scientific Laboratory where part of this work was written.

*Work supported in part by the National Science Foundation and by the City University of New York Faculty Research Award Program.

¹R. L. Burman, private communication.

²R. G. Parsons, J. S. Trefil, and S. D. Drell, *Phys. Rev.* **133**, B847 (1965).

³F. Becker and Z. Maric, *Nuovo Cimento* **41B**, 174 (1966).

⁴S. Barshay and G. E. Brown, *Phys. Lett.* **16**, 165 (1965).

⁵W. B. Kaufmann, J. C. Jackson, and W. R. Gibbs, *Phys. Rev. C* **9**, 1340 (1974).

⁶K. Bjornenak, J. Finjord, P. Osland, and A. Reitan, *Nucl. Phys.* **B20**, 327 (1970); **B22**, 179 (1970); M. A. Locci and P. Picchi, *Nuovo Cimento* **57A**, 803 (1968).

⁷E. Rost and G. W. Edwards, *Phys. Lett.* **37B**, 247 (1971).

⁸R. J. Glauber, in *Lectures in Theoretical Physics*, edited by W. Brittin *et al.* (Interscience, New York, 1959), Vol. I.

⁹V. Franco, *Phys. Rev. C* **9**, 1690 (1974).

¹⁰D. S. Koltun, in *Advances in Nuclear Physics*, edited by M. Baranger and E. Vogt (Plenum, New York, 1969), Vol. 3.

¹¹For a half-off-shell generalization, see L. C. Liu, *Nucl. Phys.* **A223**, 523 (1974).

¹²L. J. Tassie and F. C. Barker, *Phys. Rev.* **111**, 940 (1958). It may be worth mentioning that the presence of spurious states in harmonic oscillator wave functions usually complicates the treatment of the c.m. correlation when nuclear excitations are involved.

However, in this work the initial and final nuclei are taken to have the same configuration in coordinate space. Furthermore, the coherent approximation (see Sec. IV) is used. Consequently, the above mentioned complication in treating the c.m. correlation does not arise in our calculations.

¹³U. Fano and G. Racah, *Irreducible Tensorial Sets* (Academic, New York, 1959).

¹⁴H. R. Collard, L. R. B. Elton, and R. Hofstadter, in *Nuclear Radii*, edited by H. Schopper (Springer Verlag, Berlin-Heidelberg-New York, 1968), p. 32.

¹⁵P. B. Jones, *The Optical Model in Nuclear and Particle Physics* (Interscience, New York, 1963), p. 105. See also G. Fäldt, *Nucl. Phys.* **A206**, 176 (1973), and the references contained therein for other descriptions of local potentials.

¹⁶D. J. Herndon *et al.*, Lawrence Radiation Laboratory Report No. UCRL-20030, 1970 (unpublished), p. 79.

¹⁷The slow convergence of the series and the large cancellations which occur are not terribly surprising since between 100 and 400 MeV the basic πN interaction is very strong and absorptive (and is strongest and most absorptive near 180 MeV). For a discussion of the convergence properties of the multiple-scattering series as illustrated by hadron-nucleus forward elastic scattering, see V. Franco, *Phys. Rev. C* **6**, 748 (1972), where it is shown how rather large cancellations can take place in the multiple-scattering series. The large cancellations in the double charge exchange amplitude has a similar explanation. Triple scattering differs from double scattering in that col-

lisions with one core nucleon also take place. The n -fold scattering differs from double scattering in that collisions with $n-2$ core nucleons also take place. The following simplified model illustrates the general behavior of the series. If we assign some strength α to a collision between the pion and a core nucleon, the multiple-scattering series will behave like $\sum_{m=0}^{16} \binom{16}{m} \alpha^m$. The first term ($m=0$) is unity. It represents the double-scattering term, i.e., double charge exchange scattering with no collisions with any core nucleons. The next term ($m=1$) is 16α . It represents the triple scattering term, i.e., the DCE scattering with collisions with one core nucleon. Since there are 16 core nucleons in ^{18}O , we get the factor 16. The entire series sums to $(1+\alpha)^{16}$. For absorptive interactions α is negative. For a rather strong interaction α could be, for example, approximately $-\frac{1}{4}$. In this

case the triple-scattering amplitude ($m=1$) would be -4 , and the cross section for double plus triple scattering would be $(1-4)^2$, or 9 times as large as for double scattering alone. (This would be similar to the results shown in Fig. 5 near 200 MeV.) The entire series sums to $(0.75)^{16} \approx 0.01$. Although the convergence is slow, the $m=11$ term is 10^{-3} in magnitude, the $m=12$ term is 10^{-4} in magnitude, the $m=13$ term is 10^{-5} in magnitude, and the $m=16$ is 10^{-10} in magnitude; so that convergence is not in doubt. The cross section is $(0.01)^2 = 10^{-4}$, which is a factor of $\sim 10^4$ smaller than the double-scattering cross section contribution. This simplified model gives results which are in qualitative agreement with our more detailed calculations.

¹⁸See, for example, C. Wilkin, *Nuovo Cimento Lett.* 4, 491 (1970).